The University of Oklahoma

arXiv: [hep-ph] OU-HEP-251123 November 2025

Enhanced Charged Higgs Signal at the LHC

Chenyu Fang a* , Wei-Shu Hou b† , Chung Kao a‡ , Mohamed Krab b§

^aHomer L. Dodge Department of Physics and Astronomy, University of Oklahoma, Norman, OK 73019, USA ^bDepartment of Physics, National Taiwan University, Taipei 10617, Taiwan (Dated: November 26, 2025)

Abstract

We investigate the discovery prospects of a charged Higgs boson (H^{\pm}) at the Large Hadron Collider (LHC) via the process $cg \to bH^{\pm} \to bc\bar{b}$ within the framework of a general two Higgs doublet model (G2HDM). In most two Higgs doublet models, the H^+cb coupling (g_{H^+cb}) is usually suppressed by the CKM matrix element V_{cb} . In G2HDM, there are additional Yukawa couplings, the process $cg \to bH^{\pm} \to bc\bar{b}$ is enhanced by the coupling $g_{H^+cb} \simeq \rho_{tc}V_{tb}$ in both the production and decay of the charged Higgs boson. We study possible physics backgrounds and evaluate the discovery potential with realistic acceptance cuts and tagging efficiencies at collider energies of \sqrt{s} =13 and 14 TeV. We apply b-tagging and c-tagging and show that m_{H^+} can be extracted by pairing the tagged b and c-jets. Our analysis leads to promising results for the current LHC and expected high-luminosity LHC.

PACS numbers:

 $^{^{\}ast}$ E-mail address: chenyu.fang@ou.edu

 $^{^{\}dagger}$ E-mail address: wshou@phys.ntu.edu.tw

[‡] E-mail address: Chung.Kao@ou.edu

[§] E-mail address: mkrab@hep1.phys.ntu.edu.tw

I. INTRODUCTION

The discovery of the 125 GeV Higgs boson in 2012 [1, 2] marked the completion of the experimentally observed particle spectrum predicted by the electroweak theory of the Standard Model (SM) [3–5].

However, certain phenomena, such as the baryon asymmetry of the Universe [6] as well as the flavor anomalies of quarks and leptons [7, 8], indicate deviations from the SM and suggest the need for additional sources of Charge-Parity (CP) violation and extended Yukawa couplings. These discrepancies highlight the necessity of extending SM and have made the search for physics beyond the Standard Model (BSM) a primary objective of the LHC.

The general two Higgs doublet model (G2HDM) extends the SM by introducing an additional SU(2) scalar doublet. Following electroweak symmetry breaking, G2HDM gives rise to five physical Higgs bosons: two CP-even scalars $[H^0$ (heavier) and h^0 (lighter)], one CP-odd pseudoscalar (A^0) and a pair of charged Higgs bosons (H^{\pm}) . Two scalar doublets can introduce sources of CP violation [9, 10] and allow for a second set of Yukawa couplings, including extra flavor-changing couplings.

To study the interaction of $H^+\bar{c}b$, we follow the Yukawa Lagrangian present in Refs. [11, 12],

$$\mathcal{L}_{Y} = \frac{-1}{\sqrt{2}} \sum_{F=U,D,L} \bar{F} \left\{ \left[\kappa^{F} s_{\gamma} + \rho^{F} c_{\gamma} \right] h^{0} + \left[\kappa^{F} c_{\gamma} - \rho^{F} s_{\gamma} \right] H^{0} \right. \\
\left. - i \operatorname{sgn}(Q_{F}) \rho^{F} A^{0} \right\} P_{R} F - \bar{U} \left[V \rho^{D} P_{R} - \rho^{U\dagger} V P_{L} \right] D H^{+} - \bar{\nu} \left[\rho^{L} P_{R} \right] L H^{+} + \text{H.c.}, \tag{1}$$

where $P_{L,R} \equiv (1 \mp \gamma_5)/2$, $c_{\gamma} \equiv \cos \gamma$, $s_{\gamma} \equiv \sin \gamma$ with γ is the mixing angle between the two CP-even scalars H and h, and Q_F is the fermion charge. The κ^F matrices are diagonal and fixed by fermion masses to $\kappa^F = \sqrt{2} m_F/v$ with $v \approx 246$ GeV, while the ρ^F matrices contain both diagonal and off-diagonal elements that serve as free parameters. In our collider study, we choose ρ^F as real. In what follows, we drop the superscript F.

Focusing on the coupling of H^+cb one can derive the interaction Lagrangian from Eq. (1),

$$\mathcal{L}_{H^{+}\bar{c}b} = -\bar{c} \left[(V_{cd}\rho_{db} + V_{cs}\rho_{sb} + V_{cb}\rho_{bb}) P_{R} - (\rho_{uc}^{*}V_{ub} + \rho_{cc}^{*}V_{cb} + \rho_{tc}^{*}V_{tb}) P_{L} \right] b H^{+} + \text{H.c.}$$

$$\simeq \bar{c} \left[\rho_{tc}^{*}V_{tb}P_{L} \right] b H^{+} + \text{H.c.}.$$
(2)

The coupling $H^+\bar{c}b \propto \rho_{tc}V_{tb}$ is not suppressed by CKM mixing [13, 14]. In this Letter, we propose the process $cg \to bH^+$ (see Fig. 1) followed by $H^+ \to c\bar{b}$ as a promising discovery channel of the BSM charged Higgs boson at LHC in the near future. We first examine the parameter space of ρ_{tc} under the current constraints imposed on the G2HDM. We then investigate the discovery potential of the Higgs signal in the presence of SM backgrounds. By applying realistic acceptance cuts, including b-tagging and c-tagging efficiencies, we present the statistical significance at the LHC for center-of-mass energies of $\sqrt{s} = 13$ and 14 TeV.

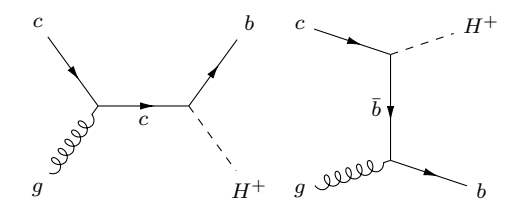


FIG. 1: Leading-order Feynman diagrams for $cg \to bH^+$.

II. HIGGS DECAYS AND LIMITS ON PARAMETERS

In this section, we utilize the latest results from Higgs measurements at the LHC and B-physics experiments to constrain the parameter space of the G2HDM. We also present the branching ratios of the dominant decay channels of the charged Higgs with different parameters.

A. Limits on ρ_{tc}

Recent searches for the flavor-changing decay $t \to ch$ by ATLAS [15] and CMS [16] collaborations have placed stringent constraints on the branching ratio with $\mathcal{B}(t \to ch) \leq 3.4 \times 10^{-4}$ [15] and $\mathcal{B}(t \to ch) \leq 3.7 \times 10^{-4}$ [16], respectively. This leads to an upper limit on the FCNH Yukawa coupling $|\lambda_{tch}|$

$$\lambda_{tch} \le 0.035 \tag{3}$$

for the effective Lagrangian,

$$\mathcal{L} = -\frac{\lambda_{tch}}{\sqrt{2}}\bar{c}th^0 + \text{H.c.}, \tag{4}$$

with the relation between λ_{tch} and the $t \to ch^0$ branching ratio [17] being

$$\lambda_{tch} \approx 1.92 \times \sqrt{\mathcal{B}(t \to ch)},$$
 (5)

where $|\lambda_{tch}| = \tilde{\rho}_{tc} c_{\gamma}$ and

$$\tilde{\rho}_{tc} \approx \sqrt{(|\rho_{tc}|^2 + |\rho_{ct}|^2)/2}.\tag{6}$$

See Ref. [18] for the exclusion bounds in the (c_{γ}, ρ_{tc}) plane.

The effective Lagrangian for H^0 and A^0 can be written as

$$\mathcal{L} = \frac{\lambda_{tcH}}{\sqrt{2}}\bar{c}tH^0 + i\frac{\lambda_{tcA}}{\sqrt{2}}\bar{c}tA^0 + \text{H.c.}, \tag{7}$$

where

$$|\lambda_{tcH}| = \tilde{\rho}_{tc} s_{\gamma} \quad \text{and} \quad |\lambda_{tcA}| = \tilde{\rho}_{tc}.$$
 (8)

In the alignment limit [19, 20], $c_{\gamma} \approx 0$ and $s_{\gamma} \approx 1$. That leads to $|\lambda_{tch}| \to 0$, while $|\lambda_{tcH}|$ is enhanced in the alignment limit, giving rise to same-sign top quark and/or triple-top final states via $cg \to tH^0 \to tt\bar{c}/tt\bar{t}$ [21, 22].

ATLAS [23] and CMS [24] direct searches for heavy Higgs bosons with flavor-changing couplings set further limits on ρ_{tc} . Without interference between H and A, CMS [24] set no exclusion limits on m_H or m_A for a coupling value $\rho_{tc} = 0.4$. When interference is included, still assuming $\rho_{tc} = 0.4$, the limits reach $m_H = 290$ GeV and $m_A = 340$ GeV. For a larger coupling, $\rho_{tc} = 1.0$, the limits extend to $m_H = 760$ GeV and $m_A = 810$ GeV at 95% confidence level (CL) [24]. ATLAS [23] excludes an H with masses m_H between 200-620 GeV at 95% CL for coupling values $\rho_{tt} = 0.4$, $\rho_{tc} = 0.2$, and $\rho_{tu} = 0.2$. For very small or vanishing ρ_{tu} , these exclusion limits become weaker [23].

Flavor constraints on ρ_{tc} are weak [25]. It is found that B_s mixing constrains $|\rho_{tc}| \lesssim 1.7$ for $m_{H^+} = 500$ GeV [25, 26]. The coupling ρ_{ct} is constrained to be $\rho_{ct} < 0.1$ [25]. In what follows, we set $\rho_{tc} = 0.4$, $\rho_{ct} = 0.05$. To be consistent with flavor constraints, we choose $\rho_{tt} = 0.2 \times (m_{H^+}/150 \text{ GeV})$ [27]. The remaining Yukawa couplings, such as, e.g., ρ_{bb} and $\rho_{\tau\tau}$, are chosen to satisfy flavor constraints. We refer to Ref. [28] for bounds on ρ_{tt} from B-physics and direct searches for $pp \to \bar{t}H^+b \to \bar{t}t\bar{b}b$ [29].

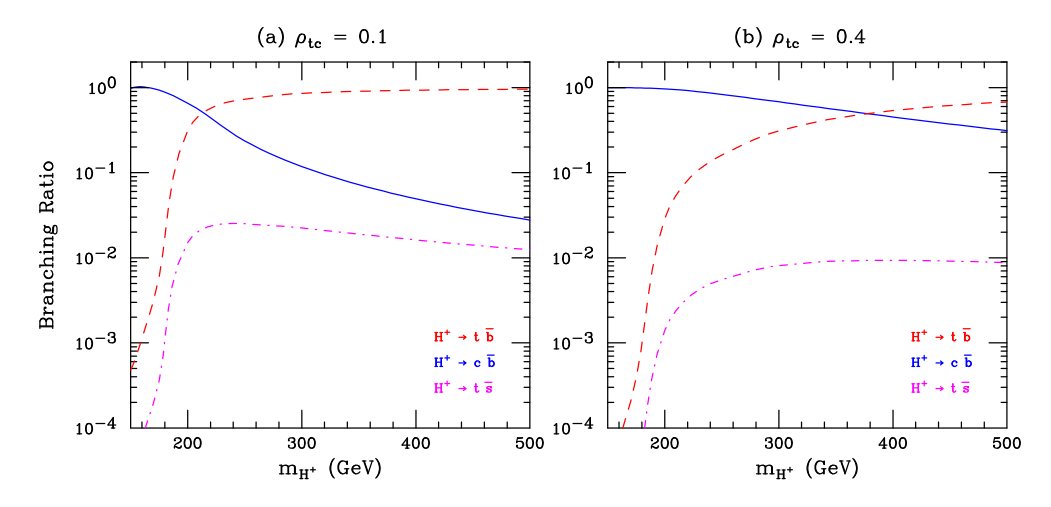


FIG. 2: Branching ratios of H^+ as a function of m_{H^+} for (a) $\rho_{tc} = 0.1$, and (b) $\rho_{tc} = 0.4$.

B. Charged Higgs decay channels

We investigate various decay channels of the charged Higgs boson H^+ , focusing specifically on $H^+ \to c\bar{b}$, $H^+ \to t\bar{b}$, and $H^+ \to t\bar{s}$. For simplicity, we assume mass degeneracy among the additional Higgs bosons, i.e. $m_H \sim m_A \sim m_{H^+}$, to forbid $H^+ \to W^+ H, W^+ A$. However, if kinematically accessible, these decays could be promising discovery channels (see, e.g., Refs. [30, 31]). The branching ratios are shown as functions of m_{H^+} for fixed values of $\rho_{tc} = 0.1$ (left) and $\rho_{tc} = 0.4$ (right) in Fig. 2. We see that while $H^+ \to c\bar{b}$ becomes the dominant decay mode as m_{H^+} less than 200 GeV for $\rho_{tc} = 0.1$ and less than 380 GeV for $\rho_{tc} \geq 0.4$, the $H^+ \to t\bar{b}$ channel remains competitive, especially for larger values of m_{H^+} .

III. HIGGS SIGNAL AND PHYSICS BACKGROUND

A. Higgs signal

We study charged Higgs boson production at the LHC via the process $cg \to bH^+$, with the subsequent decay $H^+ \to c\bar{b}$, leading to a $bc\bar{b}$ final state. The complete Monte Carlo simulation is carried out using Madgraph5_aMC@NLO [32, 33], Pythia-8 [34], and Delphes [35]. The signal cross section is evaluated using the CT14LLO parton distribution function (PDF) [36], with the renormalization and factorization scales set to $\mu_{R,F} = m_{H^+}$. Applying the above scale choices and PDF, our current estimates suggest a K-Factor of ≈ 1.95 , and is approximately the same for all three energies ($\sqrt{s} = 13, 13.6$, and 14 TeV). The K-factors are calculated using MAD-GRAPH5_AMC@NLO.

B. The Physics Background

The dominant physics background to the signal arises from $b\bar{b}j$ and $c\bar{c}j$. Using the same simulation framework and PDF as for the signal, we compute the cross sections with both the renormalization and factorization scales set to $\mu_{R,F} = \sqrt{\hat{s}}$. In addition, we scale our backgrounds to next-to-leading order using K-factor of 1.26 for $b\bar{b}j$ and $c\bar{c}j$ [33].

selection rule					
1 tagged c-jet, 2 tagged b-jets					
$p_T^j > 25 \text{ GeV}, \eta_j < 2.5, \Delta R_{jj} > 0.4$					
$p_T^{b_1} > 50 {\rm GeV}$					
$p_T^c > 70 \text{ GeV}$					
$\Delta R_{cb_1} > 2.0$					
$ M_{cb_1} - m_{H^+} \le 0.20 \times m_{H^+}$					

TABLE I: Final selection criteria for signal and backgrounds events.

C. Matching and Merging

To ensure a consistent description between matrix-element calculations from MG5, which generate hard and well-separated particles, and the parton shower in Pythia-8, which models hadronization of quarks and glouns including soft or collinear emissions. Appropriate matching and merging schemes are employed, such as the MLM and CKKW-L algorithms [37, 38]. These procedures prevent double counting of QCD emissions while preserving the correct jet multiplicity and kinematic distributions. The combination of Madgraph and Pythia-8 thus provides a complete simulation framework, yielding fully hadronized final states that realistically represent the physical signatures expected at the LHC. In our study, we adopt the MLM matching scheme with xqcut = 25 GeV for both signal and background samples.

D. Realistic Acceptance Cuts

Using the default ATLAS Delphes card, we incorporate charm-tagging efficiencies based on recent CMS results [39], with $\varepsilon_c = 0.22$, $\varepsilon_{b \to c} = 0.01$, and $\varepsilon_{j \to c} = 0.001$, where j = u, d, s, g. As for b-jet [40], the b-tagging efficiency is approximately 0.70 ($\varepsilon_b = 0.70$), the probability that a c-jet is mistagged as a b-jet is approximately 0.14 ($\varepsilon_{c \to b} = 0.14$), while the probability that a light jet (u, d, s, g) is mistagged as a b-jet is 0.01 ($\varepsilon_{j \to b} = 0.01$). For the event analysis, each event is required to contain at least three jets, including exactly one identified c-jet and two b-tagged jets.

- We adopt the following basic requirements:
- (i) exactly one c-jet with $p_T^c \ge 25$ GeV, $|\eta_c| < 2.5$; (ii) exactly two b-jets with $p_T^b \ge 25$ GeV, $|\eta_b| < 2.5$;
- (iii) angular separation between every two pairs of jets satisfy $\Delta R_{ij} \geq 0.4$.

To correctly reconstruct the events, the c-jet and one of the b-jets, denoted b_1 , must originate from the decay of the charged Higgs boson (H^+) and are expected to be energetic. In addition to the basic selection cuts, we further require $p_T^{b_1} > 50$ GeV, $p_T^c > 70$ GeV and an angular separation $\Delta R_{cb_1} > 2.0$. The invariant mass distribution of the c-jet and b_1 -jet pair, M_{cb_1} , are expected to exhibit a peak around the mass of the charged Higgs, m_{H^+} . Fig. 3 shows the $d\sigma/M_{cb_1}$ distributions for the signal with $m_{H^+} = 200$ and 400 GeV, together with the dominant physics backgrounds. A pronounced peak appears near m_{H^+} for $m_{H^+} = 200$ GeV case, while for 400 GeV the peak is less distinct, but still provides discrimination against backgrounds. Using the ATLAS mass resolution [41], the reconstructed c-jet and b_1 -jet masses are required to lie a mass window of $\Delta M_{cb_1} = 0.20 \times m_{H^+}$. These selection requirements are optimized to suppress background processes while enhancing the statistical significance of the signal. The complete set of final selection criteria is summarized in Table I.

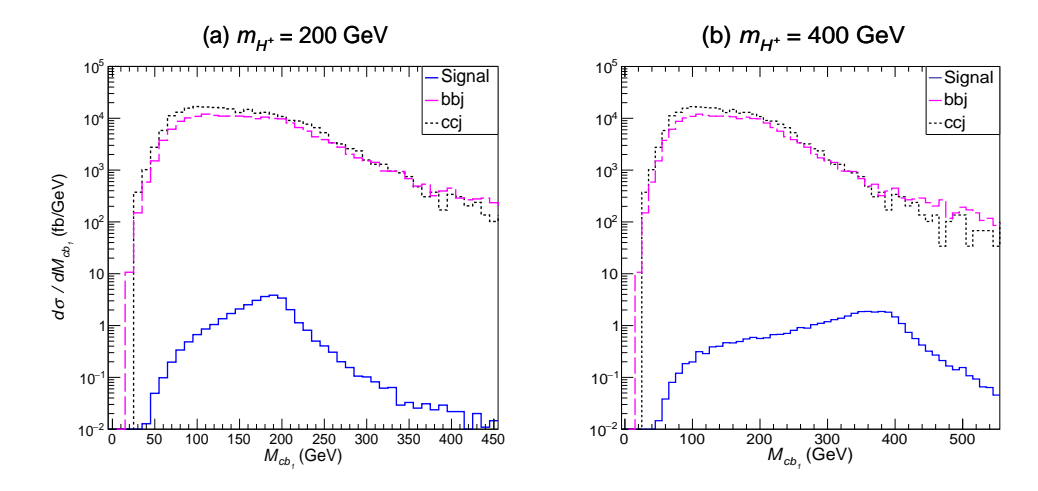


FIG. 3: Invariant mass distributions $d\sigma/dM_{cb_1}$ for the signal and dominant backgrounds $b\bar{b}j$ (magenta, dashed) and $c\bar{c}j$ (black, dotted) at $\sqrt{s}=14$ TeV, shown for $\rho_{tc}=0.4$, (a) $m_{H^+}=200$ GeV (blue, solid) and (b) $m_{H^+}=400$ GeV (blue, solid).

\sqrt{s} (TeV)	BP_1 (fb)	$b\bar{b}j$ (fb)	$c\bar{c}j$ (fb)	Total (fb)	N_{SS}
13	353.4	$8.052{ imes}10^4$	7343	$8.786{ imes}10^4$	26.6
13.6	394.0	8.407×10^4	7851	9.192×10^4	28.9
14	406.3	$8.988{ imes}10^4$	8741	$9.862{ imes}10^{4}$	28.9
\sqrt{s} (TeV)	BP_2 (fb)	$b\bar{b}j$ (fb)	$c\bar{c}j$ (fb)	Total (fb)	N_{SS}
13	103.2	8.332×10^4	7692	9.102×10^4	7.65
13.6	109.4	9.009×10^4	8223	9.831×10^{4}	7.80
14	116.1	$9.723{ imes}10^4$	9178	1.064×10^{5}	7.96
\sqrt{s} (TeV)	BP_3 (fb)	$b\bar{b}j$ (fb)	$c\bar{c}j$ (fb)	Total (fb)	N_{SS}
13	25.61	6.323×10^4	5634	6.887×10^4	2.18
13.6	27.64	$6.927{\times}10^4$	5762	$7.503{ imes}10^4$	2.26
14	29.37	7.129×10^4	7025	7.832×10^4	2.35

TABLE II: Cross sections for signal and backgrounds for $\rho_{ct} = 0.05$, $\rho_{tc} = 0.4$, $m_{H^+} = 200$ GeV (BP₁), $m_{H^+} = 300$ GeV (BP₂), and $m_{H^+} = 400$ GeV (BP₃). Statistical significance is presented with integrated luminosity L = 500 fb⁻¹. K-factors are included in the cross section.

IV. DISCOVERY POTENTIAL

After applying all selection criteria at collider energies $\sqrt{s} = 13$, 13.6, and 14 TeV, the signal cross sections for various benchmark points (BPs), along with the corresponding background cross sections, are summarized in Table II. The estimated statistical significance (N_{SS}) , calculated following Ref. [42],

$$N_{SS} = \sqrt{2(N_S + N_B)\ln(1 + N_S/N_B) - 2N_S}$$
(9)

are also presented in Table II, where N_S and N_B are number of signal and background events, respectively.

Fig. 4 presents the cross section as a function of ρ_{tc} for different values of m_{H^+} at a collider energy of $\sqrt{s} = 14$ TeV. Fig. 5 presents the 5σ discovery contour at the LHC for (a) $\sqrt{s} = 13$ TeV and (b) $\sqrt{s} = 14$ TeV in the (m_{H^+}, ρ_{tc}) plane, assuming integrated luminosities of L = 300 and 3000 fb^{-1} . The results clearly demonstrate that 14 TeV LHC with high luminosity, $L = 3000 \text{ fb}^{-1}$,

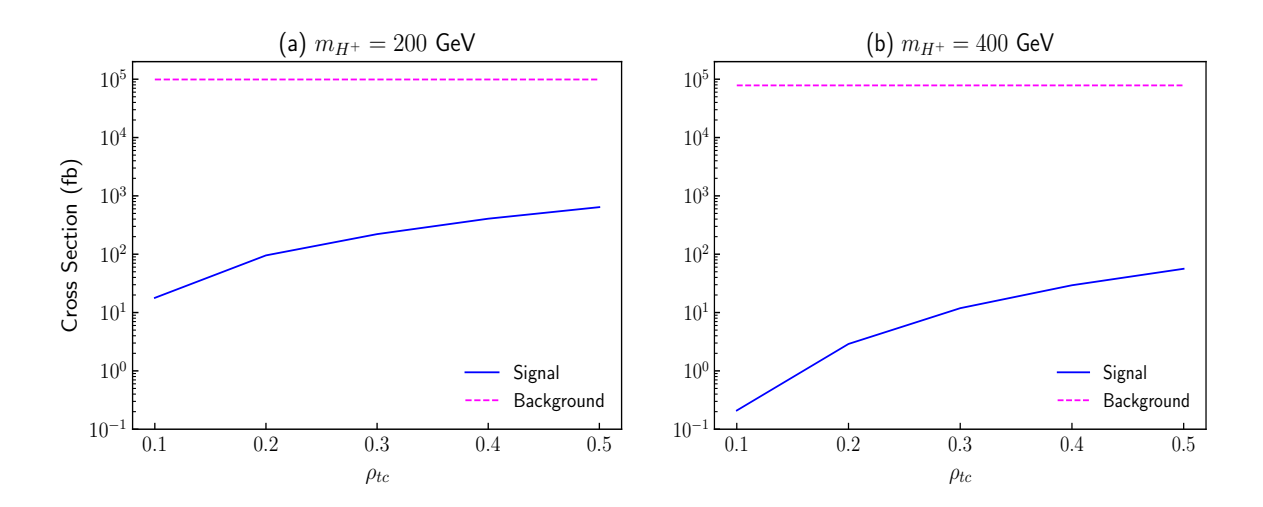


FIG. 4: The cross section as a function of ρ_{tc} for signal and background at $\sqrt{s}=14$ TeV after selection cuts, shown for (a) $m_{H^+}=200$ GeV and (b) $m_{H^+}=400$ GeV.

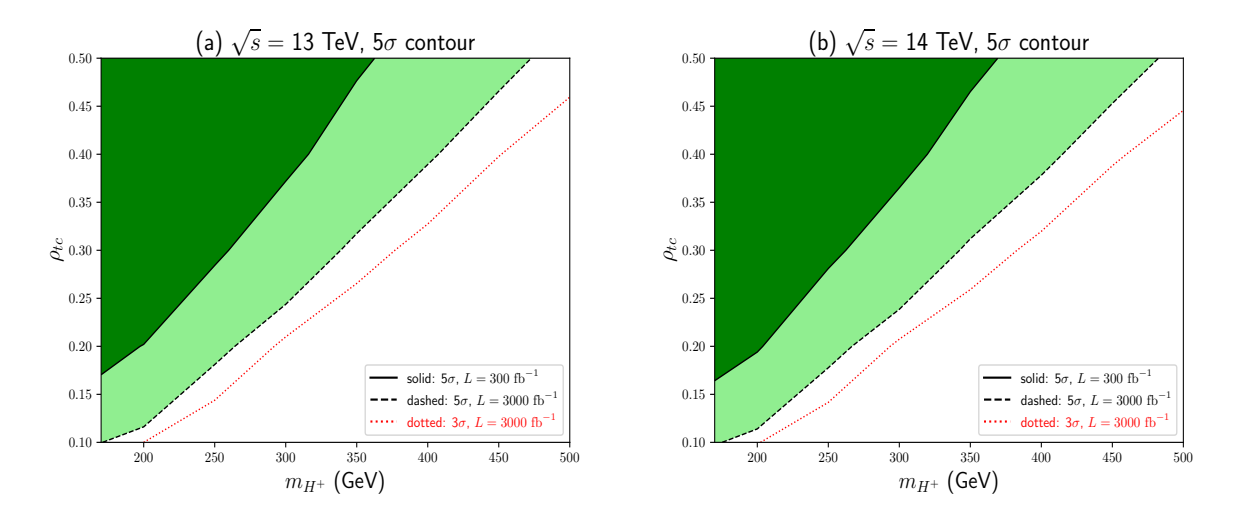


FIG. 5: The 5σ discovery contours at the LHC in the (m_{H^+}, ρ_{tc}) plane for (a) $\sqrt{s} = 13$ TeV and (b) $\sqrt{s} = 14$ TeV with L = 300 fb⁻¹ (dark green solid) and L = 3000 fb⁻¹ (light green dashed). In addition, 3σ discovery contour with L = 3000 fb⁻¹ (red dotted) are shown for both 13 and 14 TeV.

substantially enhances the discovery potential.

V. CONCLUSIONS

In the G2HDM, the process $H^+ \to c\bar{b}$ provides an excellent channel for probing the charged Higgs boson. The coupling $H^+\bar{c}b$ depends strongly on $\rho_{tc}V_{tb}$, making this process particularly sensitive to place constraints on ρ_{tc} as well. For a heavy charged Higgs boson with $m_{H^+} > m_t$, the b- and c-jets from its decay are energetic, making the signal more distinguishable from the physics backgrounds. When combined with advanced tagging techniques, the search for H^+ becomes especially promising.

We have investigated the discovery prospects at the LHC, focusing on the process $pp \to bH^+ \to bc\bar{b}$. The primary physics background comes from $b\bar{b}j$ and $c\bar{c}j$. Both signal and background

are analyzed under realistic selection criteria at collider energies of $\sqrt{s} = 13$, 13.6, and 14 TeV. According to existing constraints on the model parameters from recent studies, we evaluate the cross sections and statistical significance for various BPs, and present the corresponding discovery contours in the (m_{H^+}, ρ_{tc}) plane. Our analysis shows that, at $\sqrt{s} = 14$ TeV, the signal remains observable for $\rho_{tc} \gtrsim 0.1$ and $m_{H^+} \lesssim 450$ GeV with an integrated luminosity of L = 3000 fb⁻¹.

In summary, we have made several important contributions to the search for the charged Higgs boson:

- (i) We identify a promising production channel that is not suppressed by the CKM matrix, in contrast to two Higgs doublet models with the so-called natural flavor conservation, such as the popular 2HDM type-II.
- (ii) The signal cross section depends solely and strongly on ρ_{tc} , thereby providing a powerful method to further test the G2HDM and constrain this parameter.
- (iii) We show that m_{H^+} can be extracted by pairing the tagged b and c-jets, which provides discrimination against physics backgrounds.

Acknowledgments

CK would like to thank George Hou and the High Energy Physics Group at National Taiwan University for excellent hospitality, where part of the research was completed. This research is supported in part by the University of Oklahoma (FC and CK), the National Science and Technology Council of Taiwan under grant No. 114-2639-M-002-006-ASP (WSH and MK), and NTU grants No. 114L86001 and No. 114L891801 (WSH).

^[1] ATLAS Collaboration, G. Aad et al., Observation of a new particle in the search for the Standard Model Higgs boson with the ATLAS detector at the LHC, Phys. Lett. B 716 (2012) 1–29, [arXiv:1207.7214].

^[2] **CMS** Collaboration, S. Chatrchyan et al., Observation of a New Boson at a Mass of 125 GeV with the CMS Experiment at the LHC, Phys. Lett. B 716 (2012) 30–61, [arXiv:1207.7235].

^[3] S. L. Glashow, Partial Symmetries of Weak Interactions, Nucl. Phys. 22 (1961) 579–588.

^[4] S. Weinberg, A Model of Leptons, Phys. Rev. Lett. 19 (1967) 1264–1266.

^[5] A. Salam, Weak and Electromagnetic Interactions, Conf. Proc. C 680519 (1968) 367–377.

^[6] A. D. Sakharov, Violation of CP Invariance, C asymmetry, and baryon asymmetry of the universe, Pisma Zh. Eksp. Teor. Fiz. 5 (1967) 32–35.

^[7] **Heavy Flavor Averaging Group (HFLAV)** Collaboration, S. Banerjee et al., Averages of b-hadron, c-hadron, and τ-lepton properties as of 2023, arXiv:2411.18639.

^[8] B. Capdevila, A. Crivellin, and J. Matias, Review of semileptonic B anomalies, Eur. Phys. J. ST 1 (2023) 20, [arXiv:2309.01311].

 ^[9] S. Weinberg, Unitarity constraints on CP nonconservation in higgs-boson exchange, Phys. Rev. D 42 (Aug, 1990) 860–866.

^[10] K. Fuyuto, W.-S. Hou, and E. Senaha, Electroweak baryogenesis driven by extra top Yukawa couplings, Phys. Lett. B 776 (2018) 402–406, [arXiv:1705.05034].

^[11] S. Davidson and H. E. Haber, Basis-independent methods for the two-Higgs-doublet model, Phys. Rev. D 72 (2005) 035004, [hep-ph/0504050]. [Erratum: Phys.Rev.D 72, 099902 (2005)].

^[12] F. Mahmoudi and O. Stål, Flavor constraints on two-higgs-doublet models with general diagonal yukawa couplings, Phys. Rev. D 81 (Feb, 2010) 035016.

^[13] D. K. Ghosh, W.-S. Hou, and T. Modak, Sub-TeV H⁺ Boson Production as Probe of Extra Top Yukawa Couplings, Phys. Rev. Lett. 125 (2020), no. 22 221801, [arXiv:1912.10613].

- [14] W.-S. Hou and M. Krab, Reconstructing the general 2HDM charged Higgs boson at the LHC, Phys. Rev. D 110 (2024), no. 1 L011702, [arXiv:2405.19190].
- [15] ATLAS Collaboration, G. Aad et al., Search for flavour-changing neutral-current couplings between the top quark and the Higgs boson in multi-lepton final states in 13 TeV pp collisions with the ATLAS detector, Eur. Phys. J. C 84 (2024), no. 7 757, [arXiv:2404.02123].
- [16] CMS Collaboration, A. Hayrapetyan et al., Search for flavor-changing neutral current interactions of the top quark mediated by a Higgs boson in proton-proton collisions at 13 TeV, arXiv:2407.15172.
- [17] **ATLAS** Collaboration, G. Aad et al., Search for top quark decays $t \to qH$ with $H \to \gamma \gamma$ using the ATLAS detector, JHEP **06** (2014) 008, [arXiv:1403.6293].
- [18] M. Krab, Searching for charged Higgs bosons with flavor-changing couplings at the LHC, in 13th Large Hadron Collider Physics Conference, 8, 2025. arXiv:2508.00764.
- [19] N. Craig, J. Galloway, and S. Thomas, Searching for Signs of the Second Higgs Doublet, arXiv:1305.2424.
- [20] M. Carena, I. Low, N. R. Shah, and C. E. M. Wagner, Impersonating the Standard Model Higgs Boson: Alignment without Decoupling, JHEP 04 (2014) 015, [arXiv:1310.2248].
- [21] M. Kohda, T. Modak, and W.-S. Hou, Searching for new scalar bosons via triple-top signature in $cg \to tS^0 \to tt\bar{t}$, Phys. Lett. B 776 (2018) 379–384, [arXiv:1710.07260].
- [22] W.-S. Hou and T. Modak, Probing Top Changing Neutral Higgs Couplings at Colliders, Mod. Phys. Lett. A 36 (2021), no. 07 2130006, [arXiv:2012.05735].
- [23] ATLAS Collaboration, G. Aad et al., Search for heavy Higgs bosons with flavour-violating couplings in multi-lepton plus b-jets final states in pp collisions at 13 TeV with the ATLAS detector, JHEP 12 (2023) 081, [arXiv:2307.14759].
- [24] CMS Collaboration, A. Hayrapetyan et al., Search for new Higgs bosons via same-sign top quark pair production in association with a jet in proton-proton collisions at $\sqrt{s} = 13$ TeV, Phys. Lett. B 850 (2024) 138478, [arXiv:2311.03261].
- [25] B. Altunkaynak, W.-S. Hou, C. Kao, M. Kohda, and B. McCoy, Flavor changing heavy higgs interactions at the lhc, Physics Letters B 751 (2015) 135–142.
- [26] A. Crivellin, A. Kokulu, and C. Greub, Flavor-phenomenology of two-Higgs-doublet models with generic Yukawa structure, Phys. Rev. D 87 (2013), no. 9 094031, [arXiv:1303.5877].
- [27] W.-S. Hou, R. Jain, C. Kao, M. Kohda, B. McCoy, and A. Soni, Flavor Changing Heavy Higgs Interactions with Leptons at Hadron Colliders, Phys. Lett. B 795 (2019) 371–378, [arXiv:1901.10498].
- [28] W.-S. Hou and M. Krab, Probing the general 2HDM with flavor violation through $A \rightarrow ZH$, Phys. Rev. D 111 (2025), no. 11 115036, [arXiv:2503.23133].
- [29] **ATLAS** Collaboration, G. Aad et al., Search for charged Higgs bosons decaying into a top quark and a bottom quark at $\sqrt{s} = 13$ TeV with the ATLAS detector, JHEP **06** (2021) 145, [arXiv:2102.10076].
- [30] H. Bahl, T. Stefaniak, and J. Wittbrodt, The forgotten channels: charged Higgs boson decays to a W and a non-SM-like Higgs boson, JHEP 06 (2021) 183, [arXiv:2103.07484].
- [31] W.-S. Hou and M. Krab, Searching for resonant flavor-changing charged Higgs production at the LHC, Phys. Rev. D 111 (2025), no. 3 L031701, [arXiv:2409.18474].
- [32] J. Alwall, M. Herquet, F. Maltoni, O. Mattelaer, and T. Stelzer, MadGraph 5: Going Beyond, JHEP 06 (2011) 128, [arXiv:1106.0522].
- [33] J. Alwall, R. Frederix, S. Frixione, V. Hirschi, F. Maltoni, O. Mattelaer, H. S. Shao, T. Stelzer, P. Torrielli, and M. Zaro, The automated computation of tree-level and next-to-leading order differential cross sections, and their matching to parton shower simulations, JHEP 07 (2014) 079, [arXiv:1405.0301].
- [34] T. Sjöstrand, S. Ask, J. R. Christiansen, R. Corke, N. Desai, P. Ilten, S. Mrenna, S. Prestel, C. O. Rasmussen, and P. Z. Skands, *An introduction to PYTHIA 8.2, Comput. Phys. Commun.* **191** (2015) 159–177, [arXiv:1410.3012].
- [35] DELPHES 3 Collaboration, J. de Favereau, C. Delaere, P. Demin, A. Giammanco, V. Lemaître, A. Mertens, and M. Selvaggi, DELPHES 3, A modular framework for fast simulation of a generic collider experiment, JHEP 02 (2014) 057, [arXiv:1307.6346].
- [36] S. Dulat, T.-J. Hou, J. Gao, M. Guzzi, J. Huston, P. Nadolsky, J. Pumplin, C. Schmidt, D. Stump, and C. P. Yuan, New parton distribution functions from a global analysis of quantum chromodynamics, Phys. Rev. D 93 (2016), no. 3 033006, [arXiv:1506.07443].

- [37] M. L. Mangano, M. Moretti, F. Piccinini, and M. Treccani, Matching matrix elements and shower evolution for top-quark production in hadronic collisions, JHEP 01 (2007) 013, [hep-ph/0611129].
- [38] L. Lonnblad, Correcting the color dipole cascade model with fixed order matrix elements, JHEP 05 (2002) 046, [hep-ph/0112284].
- [39] CMS Collaboration, A. Tumasyan et al., A new calibration method for charm jet identification validated with proton-proton collision events at \sqrt{s} =13 TeV, JINST 17 (2022), no. 03 P03014, [arXiv:2111.03027].
- [40] **ATLAS** Collaboration, G. Aad et al., ATLAS b-jet identification performance and efficiency measurement with $t\bar{t}$ events in pp collisions at $\sqrt{s}=13$ TeV, Eur. Phys. J. C **79** (2019), no. 11 970, [arXiv:1907.05120].
- [41] **ATLAS** Collaboration, G. Aad et al., Measurements of Higgs bosons decaying to bottom quarks from vector boson fusion production with the ATLAS experiment at $\sqrt{s} = 13$ TeV, Eur. Phys. J. C 81 (2021), no. 6 537, [arXiv:2011.08280].
- [42] G. Cowan, K. Cranmer, E. Gross, and O. Vitells, Asymptotic formulae for likelihood-based tests of new physics, Eur. Phys. J. C 71 (2011) 1554, [arXiv:1007.1727]. [Erratum: Eur.Phys.J.C 73, 2501 (2013)].